Journal of Porous Materials (2021) 28:1881–1894
https://doi.org/10.1007/s10934-021-01129-6

A high lignin-content, ultralight, and hydrophobic aerogel for oil-water separation: preparation and characterization

Yanbin Yi[1] · Pansheng Liu[1] · Nana Zhang[1] · Magdi Elamin Gibril[1] · Fangong Kong[1,2] · Shoujuan Wang[1]

Accepted: 16 July 2021 / Published online: 27 July 2021

Abstract

This work was aimed to beneficiate biomass waste (lignin) to prepare a low-cost, ultralight, and high absorbent lignin-based aerogel via a facile and environmentally-friendly method that entailed blending of modified lignin with amine (LA) under high shear with polyvinyl alcohol (PVA) solution and followed by a freeze-drying process. Methyltriethoxy silicon (MTMS) was used as a silanization agent to improve the hydrophobicity of LA-PVA aerogel via chemical vapor deposition (CVD) reaction. The chemical and physical properties of the aerogel were then investigated using several characterization techniques such as Fourier transform infrared (FTIR) spectroscopy, elemental analysis, proton nuclear magnetic resonance (HNMR) spectroscopy, X-ray photoelectron spectroscopy (XPS), scanning electron microscopy (SEM), and thermogravimetric analysis. The hydrophobicity of the aerogels was satisfactory due to the formation of polysiloxane on the surface. The absorption capacity of oil and the organic solvent was varied between 2 and 12 times. The recycling experiments showed that after ten consecutive cycles, the separation efficiency was still above 90%, indicating a high recoverability. This was in addition to its other unique properties such as low density (0.1150 g/cm^3), high porosity (88%), and satisfactory hydrophobicity (143°). Therefore, and based on the exceptional properties of the aerogel in terms of its reusability, oil/water separation efficiency, and mechanical properties render them ideal materials for application in oily wastewater treatment.

Keywords High lignin-content · Hydrophobic aerogel · Oil/water separation

1 Introduction

In recent years, frequent oil spills in the process of oil extraction and transportation, and the discharge of oily wastewater from the industry have become one of the huge environmental problems facing the world [1]. As a result, oil-water separation materials and technologies have very important scientific significance and application prospects in environmental governance and energy recovery [2]. Among the different conventional methods for removing oil and organic contaminants from wastewater, the adsorbent method is considered the most cost-effective and environmentally friendly method that does not cause secondary pollution [3]. Currently, commonly used adsorbents include activated carbon [4], zeolite [5], wood fiber [6], polyurethane foam [7, 8], and olefin resin [9, 10]. However, most of these traditional adsorbents have several disadvantages such as low absorption, environmental incompatibility, long degradation cycles, high cost, and poor recyclability [11].

Aerogels are characterized by their lowest density, high porosity, solid material, and high absorption capacity [12]. They have been considered as good adsorbent materials for removing oil spills and attracted widespread scientific interest in this regard [13]. In recent years, aerogels based on carbon nanotubes and graphene have been developed for oil-water separation, with high absorption capacity and good recyclability [14, 15]. However, complex manufacturing technologies and expensive equipment are limiting their applications [16]. Nowadays, aerogels derived from biomass materials have attracted closer attention due to their renewability, low cost,

✉ Magdi Elamin Gibril
magdi.gibril@gmail.com

✉ Shoujuan Wang
nancy5921@163.com

[1] State Key Laboratory of Biobased Material and Green Papermaking, Key Laboratory of Pulp & Paper Science and Technology of Shandong Province/Ministry of Education, Qilu University of Technology, Shandong Academy of Sciences, Jinan 250353, China

[2] Shandong Guanghua Paper Group Co. Ltd, Feixian 273401, China

abundance, and low toxicity to humans. However, the preparation of aerogels from these materials is complex, expensive, and needs special solvents [17].

Lignin is one of the natural polymers that characteristic with a rigid, hyperbranched macromolecular structure composed of three different types of phenol units [18]. Currently, More than 1.5 billion tonnes of lignin have been generated annually as byproducts in pulp industries [19, 20]. Therefore it is imperative to find out facile methods and new technologies for lignin valorization. Unfortunately, due to the complexity of chemical structure and heterogeneity, lignin has not been utilized to its full potential [21]. Based on its chemical structure, lignin has been chemically modified for different purposes [22]. It has been modified and utilized as a hydrophobic agent [23] and natural crosslinker [24] to prepare silicone elastomers [25].

In this context, there are many reports have shown that lignin is a promising bio-phenolic for aerogel synthesis [11, 26–30]. For example, lignin was blended with melamine [31], cellulose [32], polypropylene [33, 34], and with carbon [35] to prepare oil absorbant aerogels. However, lignin aerogels are suffered from rigidity, a poor adhesive of lignin molecules, and low comprehensive strength and recoverability.

This work aimed to prepare lignin-based composite aerogels for oil-water separation. Lignin was modified through the Mannich reaction to enhance its chemical reactivity to interaction with polyvinyl alcohol (PVA) which is used as the substrate and adhesive. PVA is an important component in the aerogel composition where its abundant hydroxyl groups serve as active sites for the aerogel formation. Moreover, PVA has been used widely as adhesive materials and to prepare PVA-based aerogels which have potential use in biomedical and environmental applications due to it being non-toxic, low cost, and easy to be fabricated [36–40]. However, the hydrophilicity of PVA aerogels hinders its application in oil-water separation [41]. Aerogels of LA and PVA mixture, in a ratio of 1.5:1 respectively, were prepared by freeze-drying technique. To increase the hydrophobicity, the aerogel was modified with MTMS. Fourier transform infrared (FTIR) spectroscopy, elemental analysis, proton nuclear magnetic resonance (^{1}H NMR) spectroscopy, thermogravimetric analysis (TGA), X-ray photoelectron spectroscopy, scanning electron microscopy (SEM) techniques were used to characterize the chemical structure and morphology of the prepared aerogel. The oil-water separation efficiency and repeatability were determined through the detection of the water contact angle to study the oil-water separation effect.

2 Materials and methods

2.1 Materials

Alkali lignin (AL) was purchased from Shanghai Tixiai Chemical Industry Development Co., Ltd. Formaldehyde, diethylenetriamine (DETA), polyvinyl alcohol 1799 (PVA), methyl trimethoxy silicon (MTMS), and heptane, were purchased from Shanghai Macklin Biotechnology Co., Ltd. Isopropanol and petroleum ether, were purchased from Tianjin Fuyu Fine Chemical Co., Ltd. Toluene, chloroform, and kerosene were purchased from Yantai Far East Fine Chemical Co., Ltd.

2.2 Amination of alkali lignin

Mannich reaction was applied to modify the alkali lignin [42]. 10 g of alkali lignin was dissolved into 490 g of distilled water under magnetic stirring in a three-necked flask pre-equipped pH meter and a thermometer. DETA was added dropwise at room temperature in different ratios (1:1, 1:2, and 1:3), under stirring, and pH (9–11). The pH was adjusted using a 0.5M HCL solution and 0.5M NaOH solution. 10 g of formaldehyde solution (37%) was added slowly to the mixture. After that, the temperature was increased to 50 °C, and the reaction was continued for 4 h under stirring. The mixture of reactants was poured into an excess of isopropanol to remove the unreacted DETA and precipitate the LA. The precipitated lignin was dried at room temperature for 24 h followed by drying in an oven at 40 °C (overnight).

2.3 Preparation of LA-PVA composite aerogel

Firstly, 2 wt% of PVA was prepared by dissolving 2 g of PVA in 98 g of deionized water at 95 °C and under constant and continuous stirring (500 r/min). In the next step, 3 g of the LA was added to the PVA solution under vigorous stirring until LA was dissolved and mixed well till a homogeneous mixture was obtained. To complete the reaction, the mixture was kept at 70 °C for 3 under low stirring. Thereafter, the mixture was cooled down to room temperature, frozen at − 20 for 24 h, and then subsequently freeze-dried at a condenser temperature of − 70 °C under vacuum for 48 h to obtain LA-PVA aerogel.

2.4 Preparation of hydrophobic composite aerogel

The hydrophobicity of LA-PVA composites aerogel was enhanced by silanization reaction via chemical vapor deposition (CVD) method. typically, 1.5 mL MTMS was was placed with LA-PVA in a reactant bottle. Thereafter, the

reactant bottle was tightly sealed and placed in an oven at 80 °C for 12 h. The silanated aerogel (LA-PVA-MTMS) was taken out and placed in a vacuum oven for 24 h at 60 °C to remove the unreacted silane. The obtained aerogels were kept in a plastic container for characterization and application.

2.5 Characterizations

2.5.1 Elemental analysis

The elemental analysis of lignin, LA, composite aerogel, and silanized modified aerogel was carried out by Germany (ELEMENTARY Vario EL cube). After drying the sample, an appropriate amount (2mg) of the sample for carbon, hydrogen, oxygen, and nitrogen elements were used for elemental content analysis.

2.5.2 Fourier transform infrared (FTIR)

Use the tableting method for lignin and LA. The sample is mixed with a certain amount of potassium bromide (sample: KBr = 1:100), the mixture is crushed in-ground agate, and then moved to a tablet machine to make a transparent sheet. The composite aerogel and the salinized composite aerogel were detected using solid infrared probes. The FTIR spectra of samples were recorded on FTIR spectroscopy of Bruker (VERTEX70 FTIR, Karlsruhe, Germany).

2.5.3 Proton nuclear magnetic resonance (^{1}H NMR analysis)

Lignin and LA samples were dried at 60 °C for 24 h and then were dissolved in DMSO-d_6 with the assistant of sonication. The HNMR spectra of the samples were carried out with nuclear magnetic resonance (German Bruker).

2.5.4 X-ray Photoelectron spectrometer analysis (XPS)

After drying the sample, grind it into a fine powder with an agate mortar, then spread it evenly on the aluminum foil, and use a tablet machine to smooth it. The content of each element was analyzed by an X-ray photoelectron spectrometer (ESCALAB250Xi, Thermo Fisher Scientific, USA).

2.5.5 Thermogravimetric analysis (TGA)

The thermogravimetric analysis of the samples was carried out by TA thermogravimetric analyzer (TGA Q50 California, USA). The sample was heated from 30 to 800 °C at a rate of 10 °C per minute.

2.5.6 Mechanical performance analysis

The mechanical properties of the samples are analyzed by the texture analyzer (Stable Micro Systems, TA.XT Express-C, UK). Measure the sample's compressive strain at 30%, 40%, and 50%.

2.5.7 Density and porosity

The density (ρ) of aerogel was calculated using the following formula:

$$\rho = \frac{4m}{\pi D^2 H}$$

where ρ represents the density of aerogel ($g{\cdot}cm^{-3}$), m is the weight of the aerogel (gram), D is the diameter of the cross-section of aerogels (centimeter) and H is the height of the aerogel (centimeter).

The porosity of samples was measured by the liquid displacement method. Absolute ethanol was used as the displacement liquid since it causes no swelling or shrinkage when permeating through samples. The freeze-dried samples were immersed in ethanol for 24 h and weighed after the removal of excess ethanol [43]. The porosity of the aerogels was calculated according to the following equation:

$$\text{Porosity}(\%) = \frac{W_1 - W_2}{\rho V} \times 100\%$$

Whereas W_1 and W_2 represent the weights of the samples after and before immersion in ethanol, ρ is the density of ethanol and V is the volume of the samples.

2.5.8 Scanning electron microscope (SEM)

The apparent morphology of the samples was observed with a scanning electron microscope at an acceleration voltage of 15 kV. The samples were coated with gold- for 5 min before being tested.

2.5.9 Absorption capacity of oil and organic solvents

The absorption capacity of LA-PVA-MTMs aerogel was measured by immersing the aerogel in different kinds of solvents (including methylbenzene, petroleum ether, kerosene, n-heptane, trichloromethane, and soybean oil) for a specific time and then taken out to measure the weight of aerogel filled with liquids. The absorption capacity of oil and organic solvents was calculated by the following equation:

$$Q = (m - m_0)/m_0 \times 100\%$$

where Q, m, and m_0 represent the oil absorption capacity of the aerogel (g/g), the weight of aerogel after absorption (gram), and the weight of aerogel before absorption (gram). Each test was repeated three times to obtain an average value.

2.5.10 Water contact angle

The hydrophobicity of the aerogels was determined by using a water contact angle analyzer (OCA50, Dataphysics, Germany). In the static contact measurement, a water drop of about 2 µL was injected on the surface of the sample through the injection system of the tester. The water contact angle for aerogels was investigated using a high-resolution video collection system and analyzed with image analysis software.

2.5.11 Oil-water separation efficiency

The separation efficiency (R%), was calculated by the equation [44]:

$$R(\%) = \left(1 - C_p / C_i\right) \times 100\%$$

where C_p is oil content in water after one-time separation and C_i is the oil content in the original oil/water mixture.

2.5.12 Reusability

To evaluate the reusability of the samples we performed 10 consecutive cycles of absorption and desorption. The saturated sample was immersed in 200 mL of absolute ethanol at 70 °C for 0.5 h. The oil was completely dissolved in ethanol, and then it was separated from the resulting mixture using vacuum distillation.

3 Results and discussion

3.1 Amination of the lignin (LA)

The amination of the alkali lignin was carried out according to the method reported by Teng et al. [45], under alkaline conditions (Scheme 1) using DETA. Modified lignin (LA) was characterized by elemental analysis, FTIR, ^{1}H NMR, and XPS.

The elemental analysis was used to determine the nitrogen content of the LA and the results are placed in Table 1. It was found that the nitrogen content of LA was significantly increased as compared with that of lignin, this is ascribed to the chemical structure of DETA. Also, it was observed that the amount of DETA to lignin in the mixture affected the nitrogen content of the LA; when they were mixed in the ratio of 1:1, the nitrogen content of LA was increased up to 5%, and beyond that, there was a slight increase in the nitrogen content of LA. This phenomenon may be attributed to the near saturation of the active sites of the phenol structure of lignin [46]. The results are in good agreement with those reported in the previous literature [47, 48]. The results revealed that the highest nitrogen content (5.85%) was obtained in LA from 1:2, which was a little higher than LA from 1:1. However, the ratio 1:1 was selected for the preparation of LA in this work.

It was posted that lignin is a biomaterial and its products can degrade by the microorganisms in the soil in case their C/N ratio was lower than 20 [49]. Thus, the C/N ratios of as-prepared LA were calculated from the elemental analysis data to evaluate their biodegradable as shown in Table 1. The result displayed that the C/N ratios of all the LA were lower than 20, and were ranged between 6.07 and 12.1, that showing the LA possessed excellent biodegradability.

The chemical structural and functional groups of the lignin (L) and LA were examined by the FTIR spectra, and the obtained results are shown in Fig. 1a. It is obliviously that both curves are exhibited typical absorption peaks of lignin, for example, the peak at 3435 cm^{-1} attributed to the hydroxyl groups in both aliphatic and phenolic structures. while the peaks at 2936 cm^{-1} and 2837 cm^{-1} ascribed to the C–H asymmetrical stretching and vibrations in methyl

Table 1 Elemental analysis results of Alkali Lignin and LA

	N(%)	C(%)	H(%)	O(%)	C/N
Alkaline Lignin	0.13	51.28	4.43	31.38	—
LA(1:1)	5.10	55.46	6.84	29.77	10.875
LA(1:2)	5.85	56.05	5.80	26.50	9.581
LA(1:3)	4.96	54.72	7.76	27.04	11.032

Scheme 1 Schematic representations of the chemical reactions of amination of lignin with DETA

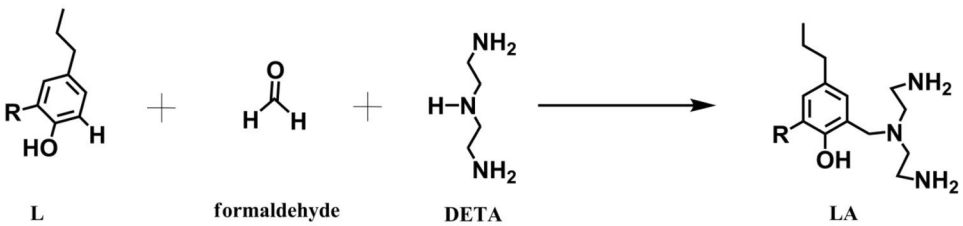

L formaldehyde DETA LA

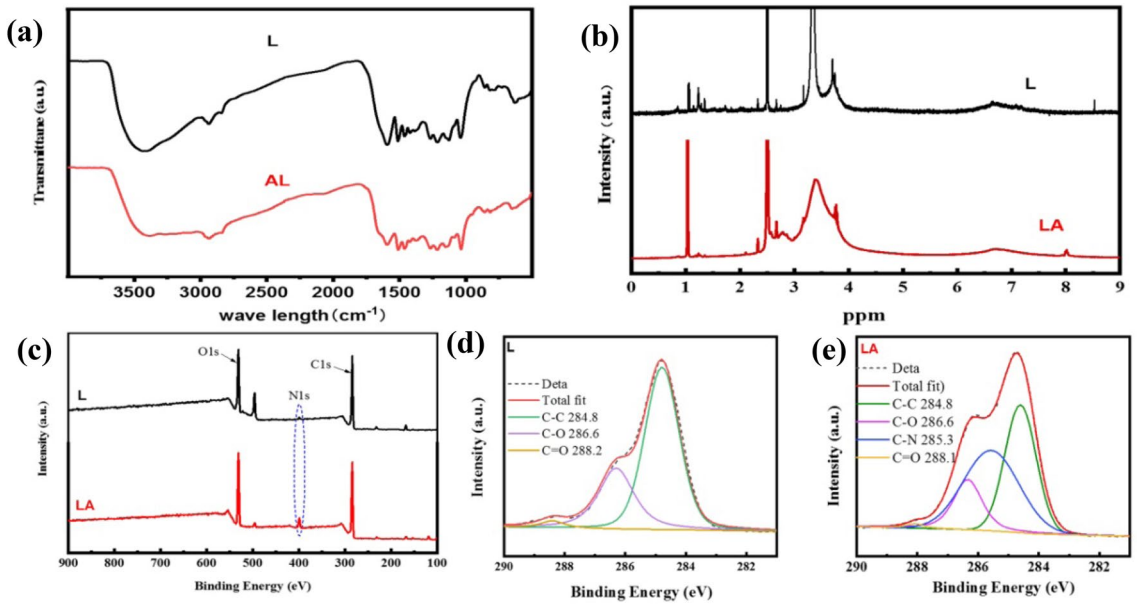

Fig. 1 The FTIR spectra (**a**), HNMR spectra (**b**) XPS spectra (**c**), and the C1s high-resolution diagrams (**d**) and (**e**) of Lignin and LA

and methylene structures, respectively. And also, the peaks at 1600 cm^{-1} and 1512 cm^{-1} are assigned to the aromatic skeletal stretching vibrations. The peaks at 1459 cm^{-1} and 834 cm^{-1} ascribed to C-H bending and vibrations, respectively [47]. After modification, there are some changes in the intensity of these peaks were observed in the FTIR spectrum of these LA. For example, the intensity of peaks at 2936 cm^{-1} and 2837 cm^{-1} originating from the C–H stretching vibrations in methyl and methylene structures became widen after modification [48]. Besides, the intensity of the peaks associated with C–H vibrations from the aromatic skeleton of lignin at 1600 cm^{-1} 1512 cm^{-1},1459 cm^{-1}, and 834 cm^{-1}, were decreased significantly in the spectra of LA. this is due to the Mannich reaction takes place at the aromatic region of lignin. Worth mention, one of the most important changes in the LA spectrum is the presence of a new peak (shoulder) at 1605 cm^{-1}, which ascribed to the N–H bending vibrations of the primary amine structure (–NH_2) [47]. It has been noting that the peaks at 1268 cm^{-1}, 1215 cm^{-1}, and at1123 cm^{-1} which are ascribed to the guaiacyl, syringyl, and ether bond in the lignin structure, were not changed this suggesting that the main structure of lignin (phenolic part) wasn't destroyed during Mannich reaction. These results are comparable with the previously reported data [42]. Hence, these changes in the LA spectrum give strong evidence of introducing the amine group into lignin as proposed in Scheme 1.

1H NMR analysis was performed to study the chemical structure and also provides more evidence about the successful introduction of amine groups. As shown in Fig. 1b, the HNMR spectrum of L showed obvious intensity signals of the aromatic proton at 6–8 ppm. Subsequently, in the HNMR spectrum of LA, these signals were reduced dramatically which implies that DETA had successfully reacted with the aromatic ring of lignin according to the Mannich reaction [50]. Besides, the new signals at 2–3 ppm, assigned to the proton of the amine group, appeared in the spectrum of LA [51]. Besides, some new signals at 2–3 ppm, assigned to the proton of the amine group, appeared in the spectrum of LA [41]. Fortunately, these changes are consistent with FTIR results and it gives another evidence of a succession of modification.

To further verify the success of the amination of lignin, the XPS analysis was applied for the elemental and chemical composition and the findings shown in Fig. 1c. The XPS spectrum of L showed distinct peaks for carbon (C1s at 284.8 eV) and oxygen (O1s at 530.7) this is due to the lignin is mainly composed of carbon, oxygen, and hydrogen. Compared to the XPS spectrum of L, the XPS spectrum of LA showed the same peaks with some differences in their intensity. Furthermore, a new peak was observed at 398.4 eV, which ascribed to the binding energy of nitrogen (N1s) [50]. The appearance of this peak indicates that the interaction between lignin and DETA was done successfully. Comparison of high-resolution C1s of XPS spectra, Fig. 1d and e, showed that the spectrum of LA exhibited a new peak at 285.3 eV which is ascribed to the C–N group originated from the interaction between lignin and DETA [52].

Arguably, the elemental analysis, FTIR, HMNR, and XPS are consistent and agreed that the amine groups were introduced successfully to lignin molecules, this modification will enhance the biodegradability and chemical reactivity

of lignin which interact with PVA easily via strong equivalent bonds.

3.2 Characterization of composite aerogel

FTIR and XPS were used to explore the functional groups and chemical structure of the synthesized aerogels. While SEM was applied to study their morphologies, and TGA to explore their thermal stability.

The elemental composition and content of the different aerogel surfaces were determined and are presented in Table 2, corresponding to the results of the XPS spectra. Compared with pure PVA aerogels, LA-PVA aerogels have new elements introduced, which are derived from the amino groups introduced in the process of aminating lignin. And the aerogel of LA-PVA-MTMS after silanization has a silicon content of 14.01%, which makes the aerogel prepared by us have a good hydrophobic effect and shows a wide range of applications in the application of oil-water separation prospect.

The morphologies of the LA-PVA, and LA-PVA-MTMS aerogels before and were observed via SEM images. As shown in Fig. 2a, b the SEM revealed that both LA-PVA (Fig. 2a) and LA-PVA-MTMS (Fig. 2b) aerogels were possessed high porous structures. These porous structures are attributed to the removed water through the frozen-drying process. this porous leads to enlarging the specific surface area of aerogels and boosts their adsorption performance [41]. Nevertheless, under high magnification, as shown in Fig. 2a, b, the surface morphology of LA-PVA was relatively smoother, whereas the surface morphology of the LA-PVA-MTMS aerogel showed some roughness (flakes) due to the presence of MTMS, which influences the wettability of the aerogel. Importantly, the 3D structure of as-prepared aerogel with a large number of porous and tunnel structures can cause the action of the capillary force and increase the specific surface area made it easy for oil to enter the aerogels i.e. promoting adsorption effeciancy [53].

The density and porosity of PVA, LA-PVA, and LA-PVA-MTMS aerogels were investigated, and the results are shown in Table 3. The density of the aerogels produced in this work classified as low density which was ranged from 0.0011 to ~ 0.5 g/cm^{-3} [54]. As it appears, the density of PVA aerogel is 0.0275g/cm^{-1}, and the porosity was 96.55%. The LA-PVA aerogel prepared by us has a density of 0.0813 g/cm^{-1} and a porosity of 88.73%. This is due to the introduction of lignin groups in aerogel lead to increase density and reduced porosity [55]. Notably, the LA-PVA-MTMS exhibited low density(0.0813 g/cm^3) which was tiny higher than those were mentioned in the literature of the ultralight aerogels, including the carbon/PVA aerogel (0.03 g/cm^3) [38], cellulose/PVA aerogel (0.013 g/cm^3) [56], boron nitrite/PVA aerogel (0.06 g/cm^3) [41], and graphene-oxide/PVA hybrid aerogel (0.2 g/cm^3) [57]. On other hand, after silanization with MTMS, the porosity of LA-PVA-MTMS was slightly decreased from 88.73% (LA-PVA) to 87.54%, this may be caused by the introduction of silane. Therefore, the

Table 2 Elemental analysis results of PVA, LA-PVA, and LA

Sample	C(%)	O(%)	N(%)	Si(%)
PVA	67.75	31.42	–	–
LA-PVA	51.95	31.47	3.22	–
LA-PVA-MTMS	49.77	27.46	3.17	14.01

Table 3 Density and porosity of PVA, LA-PVA, and LA-PVA-MTMS aerogels

Aerogel	Density(g/cm^{-3})	Porosity (%)
PVA	0.0275	96.55
LA-PVA	0.0813	88.73
LA-PVA-MTMS	0.1150	87.54

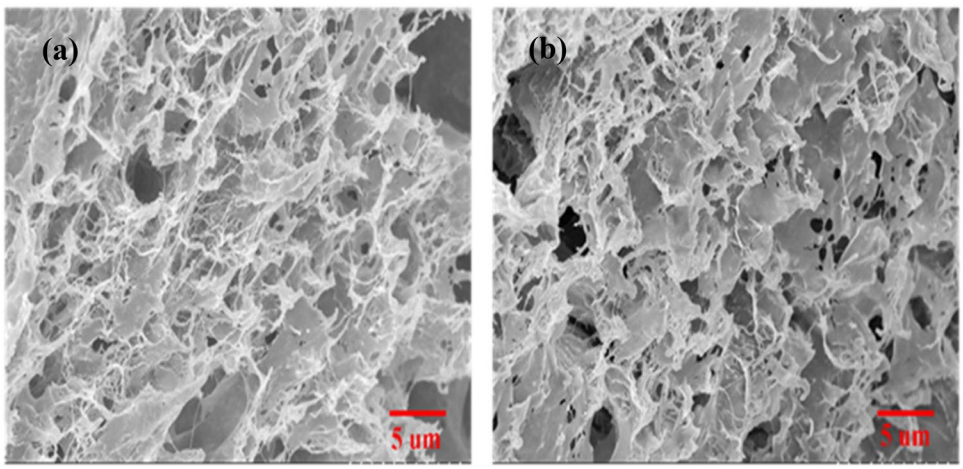

Fig. 2 The SEM image of LA-PVA (**a**) and LA-PVA-MTMS (**b**) aerogels

as-prepared aerogel, with a highly porous structure and low density, is expected to exhibit high oil absorption capacity. Interestingly, this bio-based aerogel could be easily scaled up for commercial production because of its facile and inexpensive synthesis method

The surface chemical composition of aerogels was verified by XPS analysis. As seen in the XPS plots of PVA, LA-PVA, and LA-PVA-MTMS (Fig. 3a–c.), all the spectra are shown peaks of binding energy at 286.6 and 533.2 eV which are ascribed to the C1s and O1s respectively [58]. Subsequently, in the XPS spectra of LA-PVA and LA-PVA-MTMS, the intensity of these peaks was some-changed, and new peaks were observed, these changes due to the chemical composition of lignin and MTMS [59]. The most important change was the appearance of new binding energy at 397.8 eV which is attributed to N1s in LA-PVA and LA-PVA-MTMS spectra, which confirm the existence of LA in the aerogels [50]. Importantly, the LA-PVA-MTMS spectrum showed new peaks at 149 and 100 eV, which are ascribed to the Si 2s and Si 2p, respectively [59]. This suggests that MTMS was attached to the LA-PVA aerogel successfully. Besides, there was a clear decrement of the O1s intensity of PVA after blended with LA which indicating that the interaction between PVA and LA was achieved as presupposed.

Furthermore, high-resolution elemental scans of C1s were used to confirm the interaction between LA, PVA, and MTMS. from the XPS high-resolution elemental scans of C1s, PVA (Fig 3 PVA) showed two carbon features at 283.7 eV (for CH_2) and 286.6 eV (for CH–OH). After blending with LA, the intensity of the CH-OH was decreased significantly (Fig. 3 (LA-PVA)). This is referring to the fact that "in case of hydroxyl groups of PVA is chemically involved in the irreversible reaction, the intensity of C1s (CH–OH) should be decreased clearly" [60]. Thus, arguably the interaction between PVA and LA was happening through a simple condensation reaction as proposed in Scheme 2a.

To further investigate the chemical structure of aerogels was investigated with FTIR, and the results are shown in Fig. 4a. The spectrum of pure PVA showed the main characteristic peaks of PVA at 3475, 2922, 1296, and 1072 cm^{-1} which ascribed to O–H (stretching vibration of the hydroxyl group), CH_2 (asymmetric stretching vibration), CH_3, and C–O bonds respectively. While the peaks at 1728 and 1635 cm^{-1} associated with the C=O and C=C stretching of acetate respectively [61]. For LA-PVA aerogel (Fig 4a), the FTIR spectrum showed that peaks of hydroxyl groups of PVA at 3450 cm^{-1} shift to lower wavenumber 3380 cm^{-1} due to the formation of hydrogen bonds between OH of PVA and N-H and OH of LA. The spectra of LA-PVA-MTMS showed new peaks at 1275 and 775 cm^{-1} correspondings to the Si–CH_3 bending vibration and the Si-O-Si stretching vibration respectively [62]. Also, the peak at 2922 cm^{-1} of (CH) stretching increased in intensity and shifts to a higher wavenumber and became broader after introducing MTMS. These changes are confirming the interaction between the LA-PVA and MTMS.

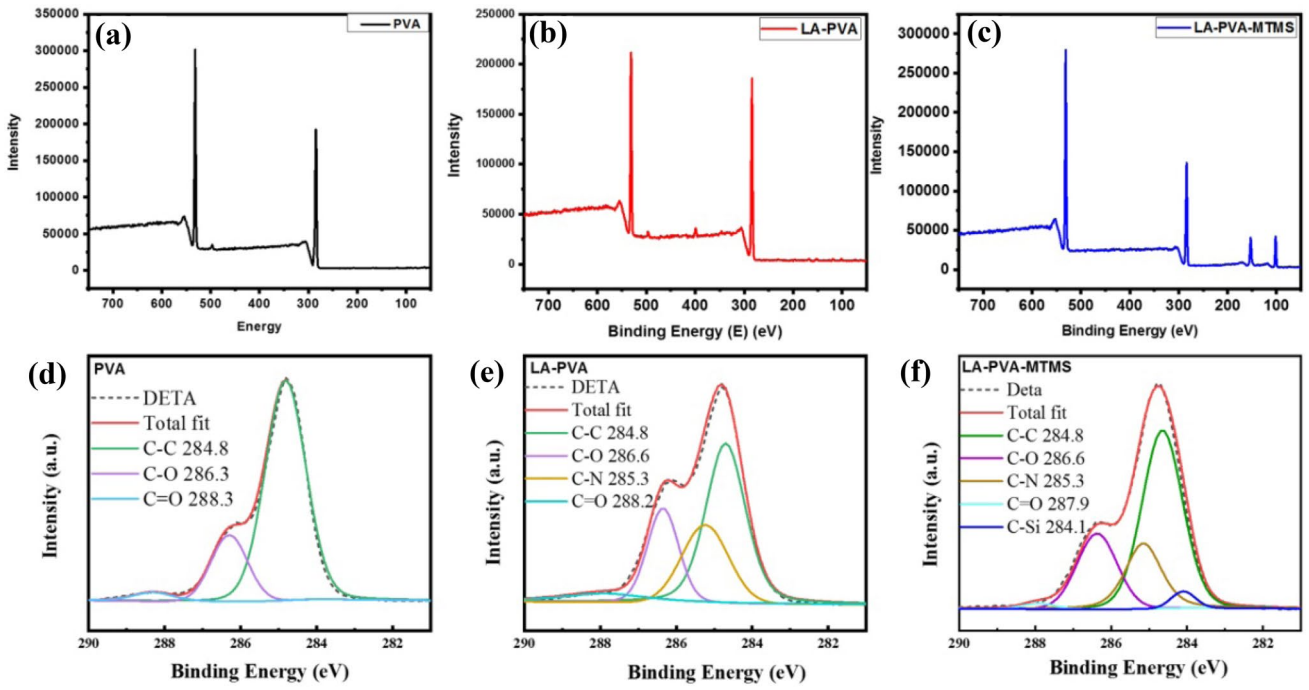

Fig. 3 The XPS spectra of PVA (**a**), LA-PVA (**b**), and LA-PVA-MTMS(c) aerogels, and the C1s high-resolution diagrams of PVA (**d**), LA-PVA (**e**), and LA-PVA-MTMS (**f**), aerogels, respectively

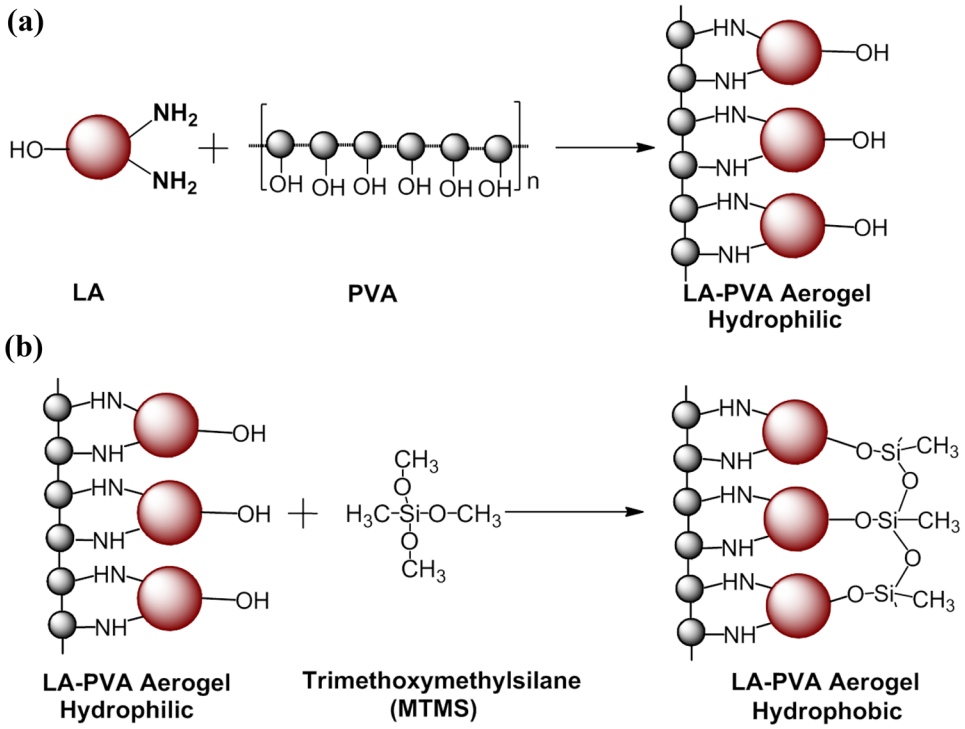

Scheme 2 Schematic representations of the chemical reactions of; **a** modified alkali lignin with PVA (LA-PVA aerogel), and **b** Silanization modification of LA-PVA aerogel with MTMS (LA-PVA-MTMS aerogel)

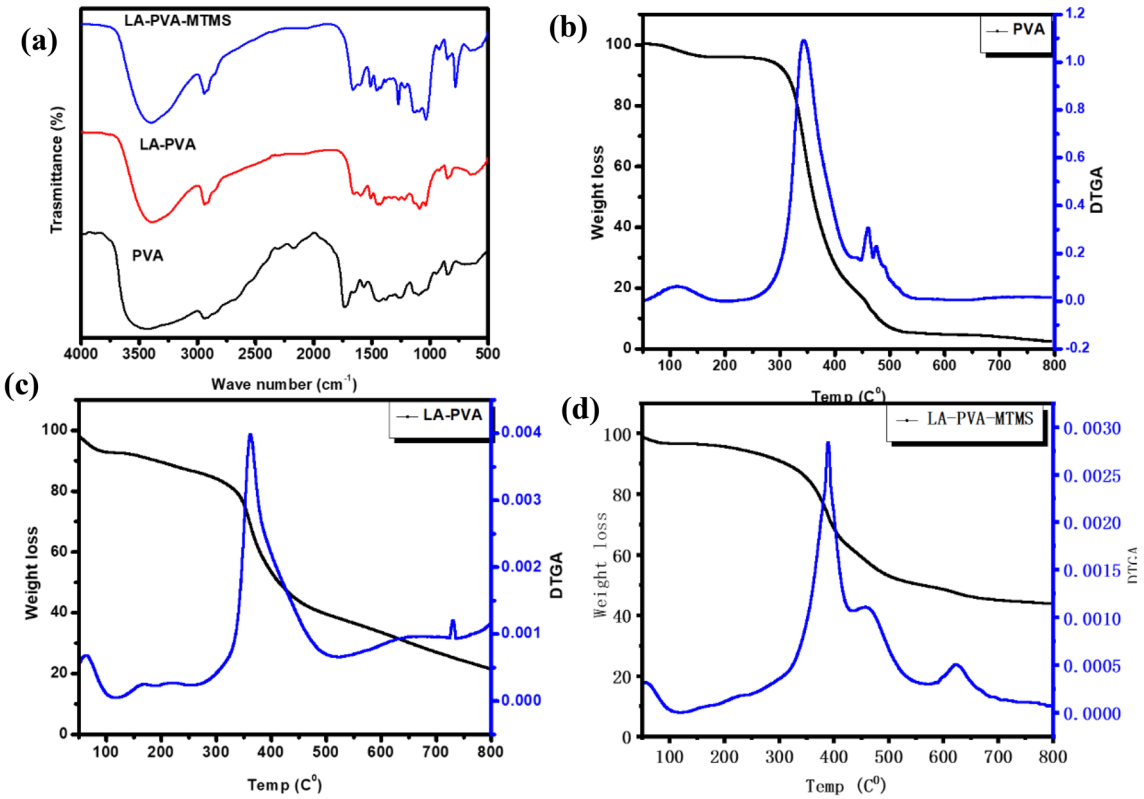

Fig. 4 The FTIR spectra **a**, TGA and DTGA spectra (**b**, **c**), and **d**) of PVA, LA-PVA, and LA-PVA-MTMS aerogels, respectively

Fig. 4b–d shows the TGA curves of the aerogels (PVA, LA-PVA, and LA-PVA-MTMS). As it is seen, all curves showed that the weight loss was divided into three main stages. At the first stage which is consists of the evaporation of the water, the aerogels were lost weight by 7 wt%. Subsequently, with the addition of the MTMS the fraction of loss in weight was decreased to 4 wt % this is due to the moisture/water content of the aerogel was reduced i.e. become more hydrophobic. The second stage of thermal degradation associates with water evaporation, chain scission, and the thermal-cracking reaction of the backbone of polymers (i.e. PVA, LA, and MTMS). The weight loss fraction underwent showed notable decrease reaching up to 61.5 wt%, and the temperature of the maximums weight loss, at this stage, was observed at 344 °C, 362°C, and 390 °C, for the PVA, LA-PVA, and LA-PVA-MTMS aerogels, respectively [63]. The increasing of maximum degradation temperature explained by the adding of LA and MTMS promoted the thermal stability of aerogels i.e. both have heat resistant properties. At the last stage, further degradation of the residual polymers to form carbon materials. The weight losses (TGA fraction) showed smaller changes under the increasing temperature. At the end of the process, the residuals quantity of the aerogels was increased significantly from 1 wt % in the case of PVA aerogel to 21 wt% and 44.5 wt% in the case of LA-PVA and LA-PVA-MTMS, respectively. This is due to the influence of LA and MTMS. The above finding out suggests that introducing MTMS to LA-PVA aerogel causing significant enhancement for the thermal property of the aerogel, and it could be used efficiently as a precursor to producing carbon aerogel [64].

To investigate the mechanical properties of the prepared aerogels, the compressive stress and strain, and their cyclic compression behaviors were measured (Fig.5). As shown in Fig. 5a, PVA aerogel, before blending with lignin, has low very elasticity properties, and it was deformed permanently when the compression strain was over 30%. The LA-PVA and LA-PVA-MTMS aerogels showed that they can both be compressed by more than 50% because of their high porosity. However, the resilience of LA-PVA and LA-PVA-MTMS aerogel has been improved to a certain extent, while their mechanical properties significantly improved (Fig. 5b and c). Under 50% compressive strain, the maximum compressive stress of LA-PVA aerogel reaches 310 KPa, while the maximum pressure of LA-PVA-MTMS aerogel reached 373 KPa. The enhancement of compression stress referring to the interior structure of aerogels and the interaction between LA, PVA, and MTMS [65]. These results are in agreement with the results reported by Zheng et al. [56]. Notably, the aerogels completely recovered their original shape with no mechanical failure after being subjected to 50% strain. Generally, the excellent mechanical property of aerogel makes it suitable for broad application prospects in the field of wastewater separation.

3.3 Absorption capacity of oil and organic solvents

Currently, scientists have an extensive research interest in polymer aerogels with high porosity. which has many advantages such as high specific surface area and high absorption performance, when it has compared to other polymer-carriers [66].

The absorption capacity oil/chemical and the oil-water separation performance of the LA- PVA-MTMS aerogel were investigated. As known, organic solvents are the main resources of water pollution that threaten the ecosystem as well as the health of humans. Herein, soybean oil and some organic solvents (including, methylbenzene, petroleum ether, kerosene, n-heptane, and trichloromethane), were selected as targeted organic pollutants. The results of oil and organic solvent absorption capacity of the LA-PVA-MTMS are shown in Fig 6. The as-prepared aerogel exhibited satisfactory absorption capacity for oil and some organic solvents as pointed in figure a, which could be as high as 2–11 times its weight. On the contrary, the absorption capacity of LA-PVA-MTMS was a little less than those prepared from blending

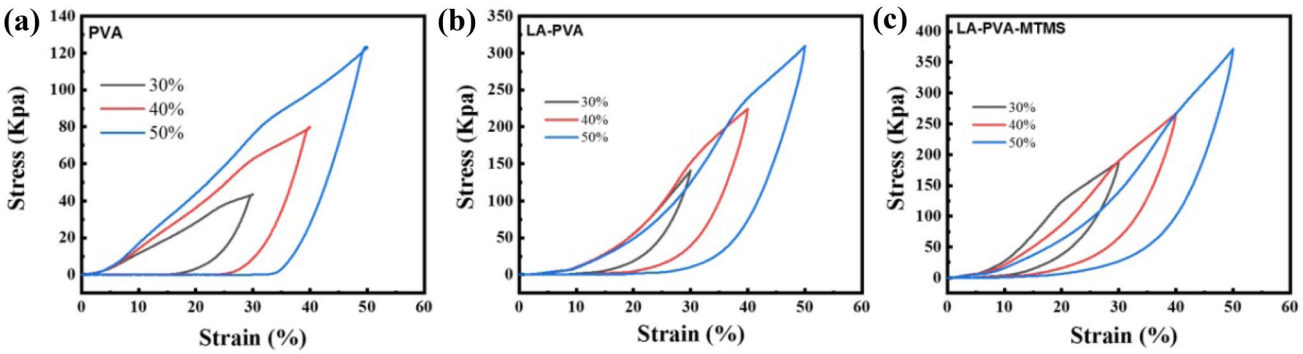

Fig. 5 Mechanical properties of the PVA (**a**), LA-PVA (**b**), and LA-PVA-MTMS (**c**) aerogels, respectively

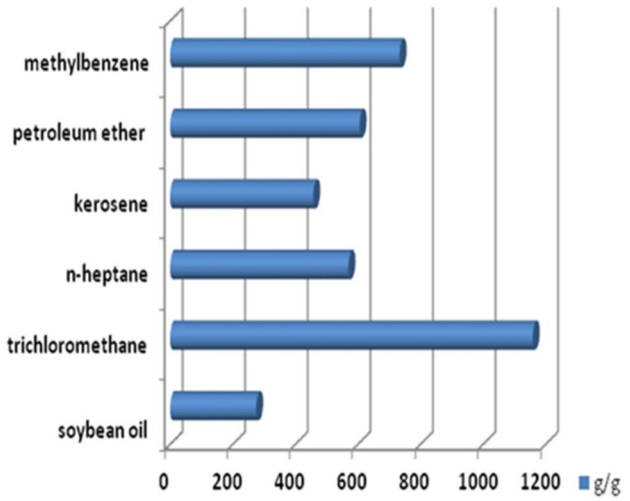

Fig. 6 The absorption capacities for various oils and organic solvents

PVA with nanocellulose [56], boron nitrite nano-sheet [41], carbon nanotube [38], and graphene [67]. However, these aerogels are limited for industrial applications due to the high cost and complicate of their synthesis. Hence, the LA-PVA-MTMS could be used as an alternative, cheap, and sustainable absorbent material for oily wastewater treatment.

3.4 Surface wettability composite aerogel

To measure the hydrophobic properties of aerogels, the water contact angle test was conducted. As known, when the water contact angle is less than 90°, the material is classified as a hydrophilic material, and when the water contact angle is greater than 90°, the material is classified as a hydrophobic material.

As shown in Fig. 7a, b, the water contact angle of the LA-PVA aerogel was 0°, and after modification with MTMS, the water contact angle of the LA-PVA-MTMS aerogel was 143°, which is an expression of high hydrophobicity. Also the Fig. 7c, d, we can observe that the drop of the colored water with methylene blue was completely absorbed by unmodified aerogel. Subsequently, after modification with MTMS, the droplets of water has stayed on the surface of the aerogel with a spherical shape and 143° of contact angle. This observation indicating that the hydrophobic aerogel was achieved successfully. Interestingly, as shown in Fig. 7e, the LA-PVA-MTMS aerogel exhibited high hydrophobicity under different pH values (pH 1, 7, 13). These results are demonstrating that the prepared aerogel has excellent separation performance under a wide range of pH, this is due to the good interaction between the aerogel's elements, high chemical durability of the aerogel's components, as well as to rough surface structure. Additionally, Fig. 7f shows that water forms droplets on the surface of the modified aerogel, and kerosene (stained with Sudan III) is quickly and completely absorbed. The result shows that the surface silanized modified composite aerogel is hydrophobic and could be effectively used for oil-water separation. Compare to the previous studies, the LA-PVA-MTMS exhibits an average of WCA up to 143°, which is higher than most of the reported hydrophobic nanocellulose/PVA aerogels, such as PVA/nanocellulose/Fe_2O_3 [68], PVA/boron nitride, PVA/nanofibers of bacterial cellulose [69], which prepared expensively. In general, the prepared aerogel exhibited a low density, high porosity, high-hydrophobicity, low-cost, and corrosion resistance, so it has expected to absorb oil and organic solvents from water effectively.

3.5 Performance of oil/water separation

The oil spill has caused serious pollution of the water environment, and the treatment of oil and organic contaminants in the water has aroused great research interest and

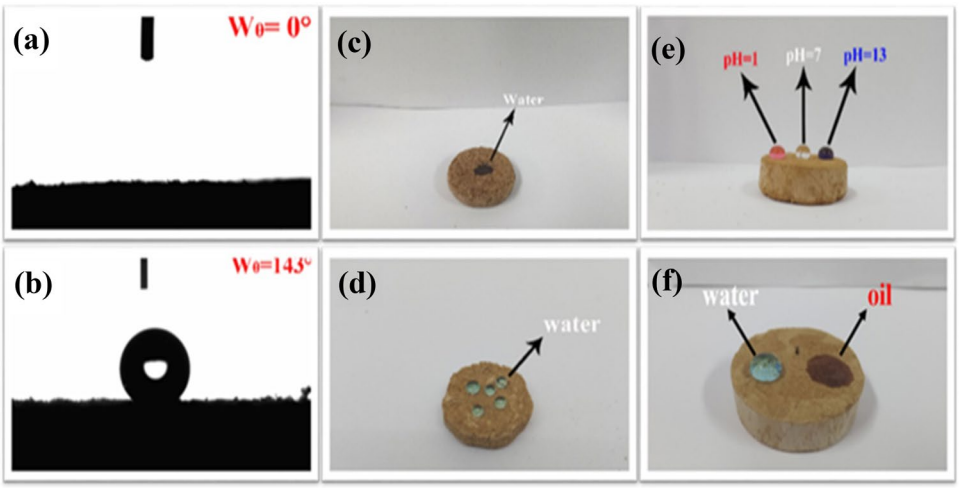

Fig. 7 The water contact angle of LA-PVA (**a**) and LA-PVA-MTMS (**b**) aerogels; The water absorption of the LA-PVA and LA-PVA-MTMS aerogels, (**c**) and (**d**) respectively; Absorption behavior of the LA-PVA-MTMS in different aqueous solutions (**e**); and A absorption behavior of the LA-PVA-MTMS aerogel (water and oil were colored by methylene blue and Sudan 3, respectively) (**f**)

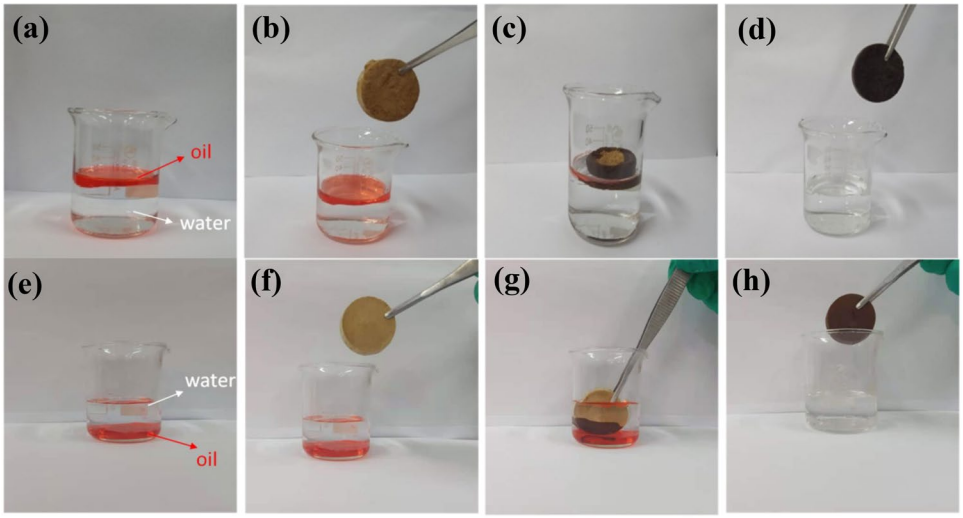

Fig. 8 **a–h** Oil absorption process of the LA-PVA-MTMS aerogel.

commercial interest among scholars. As shown in Fig.8a–h, dyed kerosene or trichloromethane with Sudan III was added into a beaker filled with water to form two lyres, and then the LA-PVA-MTMS composite aerogel was added. The dyed kerosene was absorbed totally within one minute and a clear solution (water) was left in the beaker. The results show that the modified LA-PVA-MTMS aerogel has a good adsorption capacity for oil and organic solvents as was assumed before.

To further demonstrate the absorption ability of LA-PVA-MTMS, the absorption test of aerogel for the mixture of water with oil and different kinds of organic solvents was performed to evaluate its separation efficiency. As shown in Fig.8a, the LA-PVA-MTMS aerogel showed high separation efficiency by up to 94%. This is due to the LA-PVA-MTMS has a high surface area and a large number of macroporous and microporous structures, which provides a basis for the application in oil-water separation [70].

As an important criterion for practical application, the recyclability of LA-PVA-MTMS aerogel should be seriously considered. Take toluene as a representative for absorption and explore its absorption cycle performance. As shown in Fig. 9b, after ten cycles of testing, the separation efficiency of LA-PVA-MTMS composite aerogel has been reduced to a certain extent, but it can still reach more than 90%, indicating that this composite aerogel has good performance. A certain decrease in separation efficiency was observed, this is maybe due to a certain residue of toluene during the desorption process.

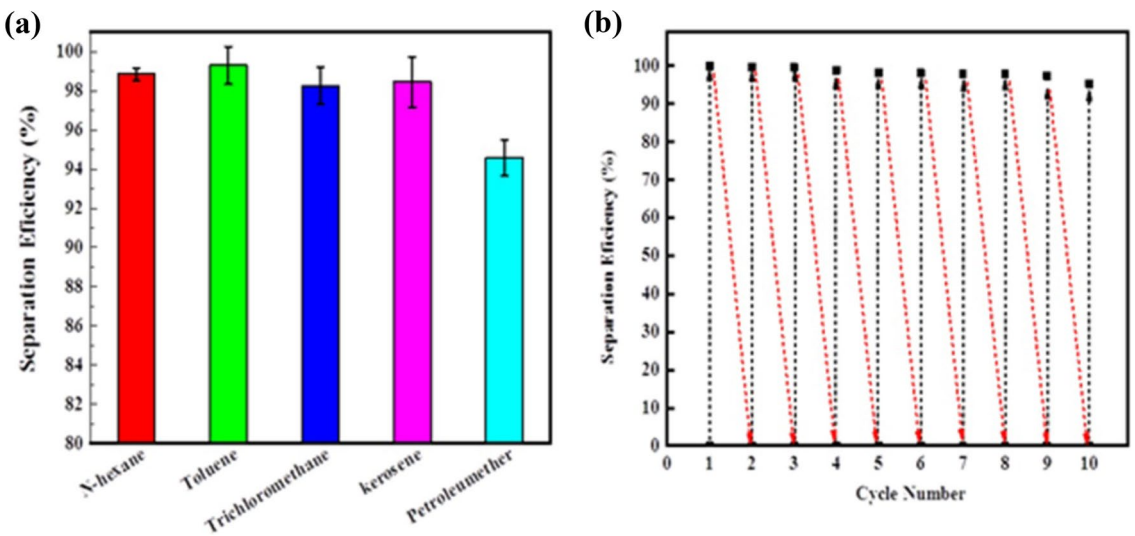

Fig. 9. The separation efficiency of different greases (**a**), Toluene recyclability test (**b**) of LA-PVA-MTMS aerogel, respectively

4 Conclusion

The successful fabrication of non-polluting, biodegradable, and environmentally friendly material, using a simple strategy may offer a model for the designing and preparation of novel materials for oil/water separation. Therefore, in this work, a facile method for fabricating lignin-based aerogels was established by cross-linking LA with PVA followed by modification with MTMS. Benefiting from the large porosity and low density of the aerogels, the prepared aerogel showed some unique properties such as low density (0.1150 g/cm^3), high porosity (88%), high hydrophobicity (143°), while maintaining its free-standing characteristics and high mechanical properties. Attributing to its porous structure, the aerogel showed a relatively high absorption capacity to various oils and chemical solvents, and it possessed excellent separation efficiency reached up to 94% in the absorption of selective oil from water in a wide range of pH. In addition to that, it exhibited good reusability (10 times). Therefore, based on the exceptional properties of the aerogel in terms of reusability, and oil/water separation efficiency, render them as ideal bio-based materials for the treatment of industrial wastewater (or oily water).

Acknowledgements The authors are grateful for the Natural Science Foundation of Shandong (No. ZR2020MC156), Shandong Key R&D Program (No. 2019JZZY010407, No. 2019JZZY010304), National Natural Science Foundation of China (Grant No. 31971605, 31800499). Key Laboratory of Bio-based Material Science & Technology (Northeast Forestry University, SWZ-MS201904), Ministry of Education Certificate of China Postdoctoral Science Foundation Grant (2019M652388), the Natural Science Foundation of Shandong (ZR2018BEM026).

References

1. H. Hu, Z. Zhao, Y. Gogotsi, J. Qiu, Compressible carbon nanotube-graphene hybrid aerogels with superhydrophobicity and superoleophilicity for oil sorption. Environ. Sci. Technol. Lett. **1**(3), 214–220 (2014). https://doi.org/10.1021/ez500021w
2. A.T. Abdulhussein, G.K. Kannarpady, A.S. Biris, One-step synthesis of a steel-polymer wool for oil-water separation and absorption. NPJ Clean Water (2019). https://doi.org/10.1038/s41545-019-0034-1
3. Z. Zhang, G. Sebe, D. Rentsch, T. Zimmermann, P. Tingaut, Ultralightweight and flexible silylated nanocellulose sponges for the selective removal of oil from water. Chem. Mater. **26**(8), 2659–2668 (2014). https://doi.org/10.1021/cm5004164
4. H. Sun, A. Li, Z. Zhu, W. Liang, X. Zhao, P. La, W. Deng, Superhydrophobic activated carbon-coated sponges for separation and absorption. ChemSusChem **6**(6), 1057–1062 (2013). https://doi.org/10.1002/cssc.201200979
5. Q. Wen, J. Di, L. Jiang, J. Yu, R. Xu, Zeolite-coated mesh film for efficient oil–water separation. Chem. Sci. **4**(2), 591–595 (2013). https://doi.org/10.1039/c2sc21772d
6. M. Likon, M. Remskar, V. Ducman, F. Svegl, Populus seed fibers as a natural source for production of oil super absorbents. J Environ. Manage **114**, 158–167 (2013). https://doi.org/10.1016/j.jenvman.2012.03.047
7. T. Zhang, L. Kong, Y. Dai, X. Yue, J. Rong, F. Qiu, J. Pan, Enhanced oils and organic solvents absorption by polyurethane foams composites modified with MnO 2 nanowires. Chem. Eng. J. **309**, 7–14 (2017). https://doi.org/10.1016/j.cej.2016.08.085
8. H. Shi, D. Shi, L. Yin, Z. Yang, S. Luan, J. Gao, J. Zha, J. Yin, R.K. Li, Ultrasonication assisted preparation of carbonaceous nanoparticles modified polyurethane foam with good conductivity and high oil absorption properties. Nanoscale **6**(22), 13748–13753 (2014). https://doi.org/10.1039/c4nr04360j
9. C. Nam, H. Li, G. Zhang, T.C.M. Chung, Petrogel: new hydrocarbon (oil) absorbent based on polyolefin polymers. Macromolecules **49**(15), 5427–5437 (2016). https://doi.org/10.1021/acs.macromol.6b01244
10. X.-M. Zhou, C.-Z. Chuai, Synthesis and characterization of a novel high-oil-absorbing resin. J. App. Polym. Sci. **115**(6), 3321–3325 (2010). https://doi.org/10.1002/app.31384
11. C. Chen, F. Li, Y. Zhang, B. Wang, Y. Fan, X. Wang, R. Sun, Compressive, ultralight and fire-resistant lignin-modified graphene aerogels as recyclable absorbents for oil and organic solvents. Chem. Eng. J. **350**, 173–180 (2018). https://doi.org/10.1016/j.cej.2018.05.189
12. H.P.S. Abdul Khalil, A.S. Adnan, E.B. Yahya, N.G. Olaiya, S. Safrida, M.S. Hossain, V. Balakrishnan, D.A. Gopakumar, C.K. Abdullah, A.A. Oyekanmi, D. Pasquini, A review on plant cellulose nanofibre-based aerogels for biomedical applications. Polymers (Basel) (2020). https://doi.org/10.3390/polym12081759
13. Y. Wang, L. Zhu, F. Zhu, L. You, X. Shen, S. Li, Removal of organic solvents/oils using carbon aerogels derived from waste durian shell. J. Taiwan Instit. Chem. Eng. **78**, 351–358 (2017). https://doi.org/10.1016/j.jtice.2017.06.037
14. S. Kabiri, D.N.H. Tran, T. Altalhi, D. Losic, Outstanding adsorption performance of graphene–carbon nanotube aerogels for continuous oil removal. Carbon **80**, 523–533 (2014). https://doi.org/10.1016/j.carbon.2014.08.092
15. H. Sun, Z. Xu, C. Gao, Multifunctional, ultra-flyweight, synergistically assembled carbon aerogels. Adv. Mater. **25**(18), 2554–2560 (2013). https://doi.org/10.1002/adma.201204576
16. H. Yagoub, L. Zhu, M. Shibraen, A.A. Altam, D.M.D. Babiker, S. Liang, Y. Jin, S. Yang, Complex aerogels generated from nanopolysaccharides and its derivatives for oil-water separation. Polymers (Basel) (2019). https://doi.org/10.3390/polym11101593
17. Y. Zhang, M. Yin, L. Li, B. Fan, Y. Liu, R. Li, X. Ren, T.-S. Huang, I.S. Kim, Construction of aerogels based on nanocrystalline cellulose and chitosan for high efficient oil/water separation and water disinfection. Carbohydr. Polym. **243**, 116461 (2020). https://doi.org/10.1016/j.carbpol.2020.116461
18. C. Jiang, H. He, H. Jiang, L. Ma, D.M. Jia, Nano-lignin filled natural rubber composites: preparation and characterization. Exp. Polym. Lett. **7**(5), 480–493 (2013). https://doi.org/10.3144/expresspolymlett.2013.44
19. R. Datta, A. Kelkar, D. Baraniya, A. Molaei, A. Moulick, R. Meena, P. Formanek, Enzymatic degradation of lignin in soil: a review. Sustainability (2017). https://doi.org/10.3390/su9071163
20. C. Xu, M. Nasrollahzadeh, M. Selva, Z. Issaabadi, R. Luque, Waste-to-wealth: biowaste valorization into valuable bio(nano) materials. Chem. Soc. Rev. **48**(18), 4791–4822 (2019). https://doi.org/10.1039/C8CS00543E
21. V.K. Garlapati, A.K. Chandel, S.P.J. Kumar, S. Sharma, S. Sevda, A.P. Ingle, D. Pant, Circular economy aspects of lignin: towards a lignocellulose biorefinery. Renew. Sustain. Energy Rev. (2020). https://doi.org/10.1016/j.rser.2020.109977

22. Y. Ge, D. Xiao, Z. Li, X. Cui, Dithiocarbamate functionalized lignin for efficient removal of metallic ions and the usage of the metal-loaded bio-sorbents as potential free radical scavengers. J. Mater. Chem. A **2**(7), 2136–2145 (2014). https://doi.org/10.1039/c3ta14333c
23. O. Gordobil, R. Herrera, Llano-Ponte, J. Labidi, Esterified organosolv lignin as hydrophobic agent for use on wood products. Prog. Org. Coat. **103**, 143–151 (2017). https://doi.org/10.1016/j.porgcoat.2016.10.030
24. J. Zhang, Y. Chen, P. Sewell, M.A. Brook, Utilization of softwood lignin as both crosslinker and reinforcing agent in silicone elastomers. Green Chem. **17**(3), 1811–1819 (2015). https://doi.org/10.1039/c4gc02409e
25. J. Zhang, Y. Ge, L. Qin, W. Huang, Z. Li, Synthesis of a lignin-based surfactant through amination, sulfonation, and acylation. J. Dispers. Sci. Technol. **39**(8), 1140–1143 (2017). https://doi.org/10.1080/01932691.2017.1385478
26. L.I. Grishechko, G. Amaral-Labat, A. Szczurek, V. Fierro, B.N. Kuznetsov, A. Pizzi, A. Celzard, New tannin–lignin aerogels. Indus. Crops Prod. **41**, 347–355 (2013). https://doi.org/10.1016/j.indcrop.2012.04.052
27. Z. Zeng, X.Y.D. Ma, Y. Zhang, Z. Wang, B.F. Ng, M.P. Wan, X. Lu, Robust lignin-based aerogel filters: high-efficiency capture of ultrafine airborne particulates and the mechanism. ACS Sustain. Chem. Eng. **7**(7), 6959–6968 (2019). https://doi.org/10.1021/acssuschemeng.8b06567
28. B.S. Yang, K.-Y. Kang, M.-J. Jeong, Preparation of lignin-based carbon aerogels as biomaterials for nano-supercapacitor. J. Korean Phys. Soc. **71**(8), 478–482 (2017). https://doi.org/10.3938/jkps.71.478
29. W. Sangchoom, R. Mokaya, Valorization of lignin waste: carbons from hydrothermal carbonization of renewable lignin as superior sorbents for CO2 and hydrogen storage. ACS Sustain. Chem. Eng. **3**(7), 1658–1667 (2015). https://doi.org/10.1021/acssuschemeng.5b00351
30. N. Ghavidel, P. Fatehi, Synergistic effect of lignin incorporation into polystyrene for producing sustainable superadsorbent. RSC Adv. **9**(31), 17639–17652 (2019). https://doi.org/10.1039/C9RA02526J
31. Y. Yang, H. Yi, C. Wang, Oil absorbents based on melamine/lignin by a dip adsorbing method. ACS Sustain. Chem. Eng. **3**(12), 3012–3018 (2015). https://doi.org/10.1021/acssuschemeng.5b01187
32. C. Wang, Y. Xiong, B. Fan, Q. Yao, H. Wang, C. Jin, Q. Sun, Cellulose as an adhesion agent for the synthesis of lignin aerogel with strong mechanical performance. Sound-absorption and thermal Insulation. Sci. Rep. **6**(1), 32383 (2016). https://doi.org/10.1038/srep32383
33. A. Alassod, S.R. Islam, A. Farooq, G. Xu, Fabrication of polypropylene/lignin blend sponges via thermally induced phase separation for the removal of oil from contaminated water. SN Appl. Sci. **2**(9), 1569 (2020). https://doi.org/10.1007/s42452-020-03372-z
34. A. Alassod, M. Gibril, S.R. Islam, W. Huang, G. Xu, Polypropylene/lignin blend monoliths used as sorbent in oil spill cleanup. Heliyon **6**(9), e04591 (2020). https://doi.org/10.1016/j.heliyon.2020.e04591
35. Y. Meng, T. Liu, S. Yu, Y. Cheng, J. Lu, H. Wang, A lignin-based carbon aerogel enhanced by graphene oxide and application in oil/water separation. Fuel **278**, 118376 (2020). https://doi.org/10.1016/j.fuel.2020.118376
36. A. Abraham, P.A. Soloman, V.O. Rejini, Preparation of chitosan-polyvinyl alcohol blends and studies on thermal and mechanical properties. Proc. Technol. **24**, 741–748 (2016). https://doi.org/10.1016/j.protcy.2016.05.206
37. J. Zhu, S. Lv, T. Yang, T. Huang, H. Yu, Q. Zhang, M. Zhu, Facile and green strategy for designing ultralight, flexible, and multifunctional PVA nanofiber-based aerogels. Adv. Sustain. Syst. **4**(4), 1900141 (2020). https://doi.org/10.1002/adsu.201900141
38. H. Zhang, J. Zhang, The preparation of novel polyvinyl alcohol (PVA)-based nanoparticle/carbon nanotubes (PNP/CNTs) aerogel for solvents adsorption application. J. Colloid Interface Sci. **569**, 254–266 (2020). https://doi.org/10.1016/j.jcis.2020.02.053
39. H.M. Kim, Y.J. Noh, J. Yu, S.Y. Kim, J.R. Youn, Silica aerogel/polyvinyl alcohol (PVA) insulation composites with preserved aerogel pores using interfaces between the superhydrophobic aerogel and hydrophilic PVA solution. Comp. Part A: Appl. Sci. Manuf. **75**, 39–45 (2015). https://doi.org/10.1016/j.compositesa.2015.04.014
40. C. Simón-Herrero, L. Gómez, A. Romero, J.L. Valverde, L. Sánchez-Silva, Nanoclay-based PVA aerogels: synthesis and characterization. Indus. Eng. Chem. Res. **57**(18), 6218–6225 (2018). https://doi.org/10.1021/acs.iecr.8b00385
41. R. Zhang, W. Wan, L. Qiu, Y. Wang, Y. Zhou, Preparation of hydrophobic polyvinyl alcohol aerogel via the surface modification of boron nitride for environmental remediation. Appl. Surface Sci. **419**, 342–347 (2017). https://doi.org/10.1016/j.apsusc.2017.05.044
42. W. Zhou, F. Chen, H. Zhang, J. Wang, Preparation of a polyhydric aminated lignin and its use in the preparation of polyurethane film. J. Wood Chem. Technol. **37**(5), 323–333 (2017). https://doi.org/10.1080/02773813.2017.1299185
43. J. Li, Y. Wang, L. Zhang, Z. Xu, H. Dai, W. Wu, Nanocellulose/gelatin composite cryogels for controlled drug release. ACS Sustain. Chem. Eng. **7**(6), 6381–6389 (2019). https://doi.org/10.1021/acssuschemeng.9b00161
44. N. Lv, X. Wang, S. Peng, L. Luo, R. Zhou, Superhydrophobic/superoleophilic cotton-oil absorbent: preparation and its application in oil/water separation. RSC Adv. **8**(53), 30257–30264 (2018). https://doi.org/10.1039/c8ra05420g
45. X. Teng, H. Xu, W. Song, J. Shi, J. Xin, W.C. Hiscox, J. Zhang, Preparation and properties of hydrogels based on PEGylated lignosulfonate amine. ACS Omega **2**(1), 251–259 (2017). https://doi.org/10.1021/acsomega.6b00296
46. P. Liu, N. Zhang, Y. Yi, M.E. Gibril, S. Wang, F. Kong, Effect of lignin-based monomer on controlling the molecular weight and physical properties of the polyacrylonitrile/lignin copolymer. Int. J. Biol. Macromol. **164**, 2312–2322 (2020). https://doi.org/10.1016/j.ijbiomac.2020.08.119
47. G.-J. Jiao, P. Peng, S.-L. Sun, Z.-C. Geng, D. She, Amination of biorefinery technical lignin by Mannich reaction for preparing highly efficient nitrogen fertilizer. Int. J. Biol. Macromol. **127**, 544–554 (2019). https://doi.org/10.1016/j.ijbiomac.2019.01.076
48. N. Zhang, S. Wang, M.E. Gibril, F. Kong, The copolymer of polyvinyl acetate containing lignin-vinyl acetate monomer: Synthesis and characterization. Eur. Polym. J. **123**, 109411 (2020). https://doi.org/10.1016/j.eurpolymj.2019.109411
49. D. Meier, V. Zúñiga-Partida, F. Ramírez-Cano, N.-C. Hahn, O. Faix, Conversion of technical lignins into slow-release nitrogenous fertilizers by ammoxidation in liquid phase. Bioresour. Technol. **49**(0960–8524), 121–128 (1994)
50. N. Zhang, S. Wang, M.E. Gibril, F. Kong, The copolymer of polyvinyl acetate containing lignin-vinyl acetate monomer: Synthesis and characterization. Eur. Polym. J. (2020). https://doi.org/10.1016/j.eurpolymj.2019.109411
51. G.J. Jiao, P. Peng, S.L. Sun, Z.C. Geng, D. She, Amination of biorefinery technical lignin by Mannich reaction for preparing highly efficient nitrogen fertilizer. Int. J. Biol. Macromol. **127**, 544–554 (2019). https://doi.org/10.1016/j.ijbiomac.2019.01.076

52. M. Li, C. Bian, G. Yang, X. Qiang, Facile fabrication of water-based and non-fluorinated superhydrophobic sponge for efficient separation of immiscible oil/water mixture and water-in-oil emulsion. Chem. Eng. J. **368**, 350–358 (2019). https://doi.org/10.1016/j.cej.2019.02.176
53. F. Ren, Z. Li, W.-Z. Tan, X.-H. Liu, Z.-F. Sun, P.-G. Ren, D.-X. Yan, Facile preparation of 3D regenerated cellulose/graphene oxide composite aerogel with high-efficiency adsorption towards methylene blue. J. Colloid Interface Sci. **532**, 58–67 (2018). https://doi.org/10.1016/j.jcis.2018.07.101
54. P. Gupta, B. Singh, A.K. Agrawal, P.K. Maji, Low density and high strength nanofibrillated cellulose aerogel for thermal insulation application. Mater. Design **158**, 224–236 (2018). https://doi.org/10.1016/j.matdes.2018.08.031
55. M.A. Karaaslan, J.F. Kadla, F.F. Ko, Lignin-Based Aerogels. In: Lignin in Polymer Composites, ed. By O. Faruk, M. Sain (Elsevier Academic Press: Amsterdam, Netherland 2016), P. 67–93
56. Q. Zheng, Z. Cai, S. Gong, Green synthesis of polyvinyl alcohol (PVA)–cellulose nanofibril (CNF) hybrid aerogels and their use as superabsorbents. J. Mater. Chem. A **2**(9), 3110–3118 (2014). https://doi.org/10.1039/C3TA14642A
57. A. Javadi, Q. Zheng, F. Payen, A. Javadi, Y. Altin, Z. Cai, R. Sabo, S. Gong, Polyvinyl alcohol-cellulose nanofibrils-graphene oxide hybrid organic aerogels. ACS Appl. Mater. Interfaces **5**(13), 5969–5975 (2013). https://doi.org/10.1021/am400171y
58. P. Liu, N. Zhang, Y. Yi, M.E. Gibril, S. Wang, F. Kong, Effect of lignin-based monomer on controlling the molecular weight and physical properties of the polyacrylonitrile/lignin copolymer. Int. J. Biol. Macromol. **164**, 2312–2322 (2020). https://doi.org/10.1016/j.ijbiomac.2020.08.119
59. F. Xue, D. Jia, Y. Li, X. Jing, Facile preparation of a mechanically robust superhydrophobic acrylic polyurethane coating. J. Mater. Chem. A **3**(26), 13856–13863 (2015). https://doi.org/10.1039/c5ta02780b
60. E. Rynkowska, K. Fatyeyeva, S. Marais, J. Kujawa, W. Kujawski, Chemically and thermally crosslinked PVA-based membranes: effect on swelling and transport behavior. Polymers **11**(11), 1799 (2019). https://doi.org/10.3390/polym11111799
61. P.K. Khanna, N. Singh, S. Charan, V.V.V.S. Subbarao, R. Gokhale, U.P. Mulik, Synthesis and characterization of Ag/PVA nanocomposite by chemical reduction method. Mater. Chem. Phys. **93**(1), 117–121 (2005). https://doi.org/10.1016/j.matchemphys.2005.02.029
62. K.S. Schlufter, Hans-peter dorn, susann heinze, thomas: efficient homogeneous chemical modification of bacterial cellulose in the ionic liquid 1-N-butyl-3-methylimidazolium chloride. Macromol. Rapid Commun. **27**(19), 1670–1676 (2006). https://doi.org/10.1002/marc.200600463
63. Z. Liu, R. Liu, Y. Yi, W. Han, F. Kong, S. Wang, Photocatalytic degradation of dyes over a xylan/PVA/TiO2 composite under visible light irradiation. Carbohydr Polym **223**, 115081 (2019). https://doi.org/10.1016/j.carbpol.2019.115081
64. S. Wang, Y. Sun, F. Kong, G. Yang, P. Fatehi, Preparation and characterization of lignin-acrylamide copolymer as a paper strength additive. BioResources (2016). https://doi.org/10.15376/biores.11.1.1765-1783
65. L. Zhou, S. Zhai, Y. Chen, Z. Xu, Anisotropic cellulose nanofibers/polyvinyl alcohol/graphene aerogels fabricated by directional freeze-drying as effective oil adsorbents. Polymers **11**(4), 712 (2019)
66. C. Daniel, W. Navarra, V. Venditto, O. Sacco, V. Vaiano, Nanoporous polymeric aerogels–based structured photocatalysts for the removal of organic pollutant from water under visible or solar light. In: Visible Light Active Structured Photocatalysts for the Removal of Emerging Contaminants, ed. By O. Sacco, V. Vaiano (Elsevier Academic Press, 2020), P. 99–120
67. Y. Chen, L. Yang, S. Xu, S. Han, S. Chu, Z. Wang, C. Jiang, Ultralight aerogel based on molecular-modified poly(m-phenylenediamine) crosslinking with polyvinyl alcohol/graphene oxide for flow adsorption. RSC Adv. **9**(40), 22950–22956 (2019). https://doi.org/10.1039/C9RA04207E
68. Z. Xu, X. Jiang, H. Zhou, J. Li, Preparation of magnetic hydrophobic polyvinyl alcohol (PVA)–cellulose nanofiber (CNF) aerogels as effective oil absorbents. Cellulose **25**(2), 1217–1227 (2018). https://doi.org/10.1007/s10570-017-1619-9
69. H. Sai, R. Fu, L. Xing, J. Xiang, Z. Li, F. Li, T. Zhang, Surface modification of bacterial cellulose aerogels' web-like skeleton for oil/water separation. ACS Appl. Mater. Interfaces **7**(13), 7373–7381 (2015). https://doi.org/10.1021/acsami.5b00846
70. Z. Xue, Y. Cao, N. Liu, L. Feng, L. Jiang, Special wettable materials for oil/water separation. J. Mater. Chem. A **2**(8), 2445–2460 (2014). https://doi.org/10.1039/C3TA13397D